ISSN 2411-3336; e-ISSN 2541-9404

JOURNAL OF MINING INSTITUTE
Zapiski Gornogo instituta
Journal homepage: pmi.spmi.ru



Research article *Geology*

Metacarbonate rocks of the Paleoproterozoic Khapchan series (southeastern part of the Anabar Shield): mineral and chemical composition, metamorphic conditions

Ekaterina Yu. Akimova✉[1], **Nikolai I. Gusev**[2,3], **Aleksandr D. Savelev**[1,2], **Daniil R. Donchenko**[1]
[1] *Saint Petersburg State University, Saint Petersburg, Russia*
[2] *All-Russian Geological Research Institute of A.P.Karpinsky, Saint Petersburg, Russia*
[3] *Institute of Precambrian Geology and Geochronology RAS, Saint Petersburg, Russia*

***How to cite this article*:** Akimova E.Yu., Gusev N.I., Savelev A.D., Donchenko D.R. Metacarbonate rocks of the Paleoproterozoic Khapchan series (southeastern part of the Anabar Shield): mineral and chemical composition, metamorphic conditions. Journal of Mining Institute. 2025. Vol. 274. N 16493, p. 3-20.

Abstract
The mineral composition of metacarbonate rocks (silicate marbles and carbonate-silicate rocks) of the Khapchan series (southeastern part of the Anabar Shield) was studied, and the *PT* (pressure and temperature)-parameters of their formation were established. Silicate marbles contain calcite, dolomite, forsterite, clinohumite, spinel, enstatite, diopside, pargasite, meionite, phlogopite, and feldspars. Carbonate-silicate rocks are composed of calcite, quartz, feldspars, diopside, grossular, marialite, and vesuvianite. Carbonate-silicate rocks are significantly enriched in SiO_2, Al_2O_3, FeO, Na_2O, K_2O, TiO_2 and contain less MgO, CaO than silicate marbles. A difference was revealed in *PT*-parameters determined for silicate marbles (temperatures 700-900 °C and pressure no more than 8 kbar) and for carbonate-silicate rocks (temperatures 680-820 °C, pressures 8-15 kbar). Silicate marbles have a primary sedimentary nature, as evidenced by their rare-element composition and the presence of fragments of host terrigenous rocks. There is no doubt about the primary sedimentary nature of carbonate-silicate rocks, which are very similar in REE distribution spectra and in rare-element composition to silicate marbles. A number of features indicate that metacarbonate rocks have undergone metasomatic alteration. Thus, in silicate marbles, reaction rims are observed around orthopyroxene, forsterite, potassium feldspar, as well as quartz veins bordered by accumulations of phlogopite, feldspars, and diopside. In carbonate-silicate rocks, the development of secondary marialite on potassium feldspar has been established; the rare-element composition of garnet may indicate its metasomatic origin.

Keywords
metacarbonate rocks; Anabar Shield; Khapchan series; metamorphism; metasomatism; *PT*-parameters; mineral geochemistry

Funding
The study was supported by the Russian Science Foundation grant N 23-27-00098.

Received: 15.05.2024 ***Accepted: 07.11.2024*** ***Online: 14.04.2025*** ***Published: 25.08.2025***

Introduction

Metacarbonate rocks are known in many Precambrian metamorphic complexes. The study of deeply metamorphosed terrigenous and carbonate rocks allows us to obtain information about their origin, sedimentation features and, more broadly, about the paleogeodynamic conditions of the formation of early Precambrian complexes [1]. However, the origin of carbonate-silicate rocks often remains controversial, which complicates the reconstruction of the geological history of metamorphic complexes. Within the Siberian Craton, metacarbonate rocks are widespread in the Proterozoic Khapchan series of the Anabar Shield [2]. They are represented in the form of lenses, interlayers of carbonate-silicate rocks and silicate marbles.

This is an open access article under the CC BY 4.0 license

The first objective of this work was a detailed study of the chemical and mineral composition of the metacarbonate rocks of the Khapchan series in order to reconstruct the conditions of their metamorphism. This objective is relevant, in particular, due to the fact that evidence of high-temperature and high-pressure metamorphism in rocks is revealed only in the process of detailed petrographic analysis [3].

The second task was to study the distribution of rare and rare earth elements (REE) in minerals of metacarbonate rocks. Rare and rare earth elements are widely used in reconstructing the formation conditions of minerals of various genesis, such as garnet [4, 5], zircon [6-8], and a number of others.

Geology

The Anabar Shield is a ledge of the deeply eroded basement of the Siberian Craton. Most of it is composed of rocks of the granulite facies of metamorphism [2]. The Anabar Shield consists of three large blocks (terranes), two of which are Archean: Magan tonalite-trondhjemite-gneiss in the west and Daldyn granulite-orthogneiss in the central part; as well as the Khapchan metacarbonate-metagraywacke Paleoproterozoic sedimentogenic belt in the east [2]. The terranes are separated by the Kotuikan-Monkholin and Saltakh-Billyakh suture (melange) zones (Fig.1). Until recently, the Khapchan series of the Khapchan belt were divided into the Khaptasynnakh and Bilekh-Tamakh strata [9] of similar lithological composition, the mapping of which is difficult. The use of geophysical data, as well as a number of new studies [10, 11] have made it possible to rethink the division of strata. At present, according to the results of compiling a new generation of the state map at a scale of 1:200,000, two series are distinguished in the structure of the Khapchan belt:

• The lower (Khardakh) series is represented by metamagmatic rocks: mesocratic and leucocratic two-pyroxene and orthopyroxene gneisses of the granulite facies of metamorphism. Magmatic formations are interpreted as part of a metamorphosed juvenile Paleoproterozoic suprasubduction complex [10]. For some granulites, it was possible to establish that their protoliths were represented by diorites of the tholeiitic series with an age of 2,095±10 million years and tonalites of the calc-alkaline series with an age of 2,030±17 million years.

• The upper (Khapchan) series is composed of metasedimentary rocks, mainly garnet and sillimanite gneisses (45-55 %), calc-silicate rocks (30-40 %), marbles and carbonate-silicate rocks (5-15 %). Metacarbonate rocks are typical for the lower part of the section (Khaptasynnakh sequence), while the upper part (Bilekh-Tamakh sequence) is almost entirely composed of garnet gneisses. The alternation of carbonate rocks and graywackes in the stratigraphic sections is explained by the influx of material from different sources, which was controlled by tectonic activity in the region [12].

The metacarbonate rocks of the Khaptasynnakh sequence form a series of lenticular layers reaching a thickness of 100-250 m, represented by carbonate-silicate rocks and silicate marbles. Based on the correlation of sections, the Khapchan series contains five metacarbonate packs, four of which belong to the Khaptasynnakh sequence, and the fifth, represented by rare interlayers, belongs to the upper Bilekh-Tamakh sequence. Marbles and calc-silicate rocks form horizons with a thickness from several meters in the lower part of the Khapchan series to several hundred meters in its middle part [12]. Carbonate-silicate rocks and silicate marbles differ in the percentage of silicate minerals and quartz. Externally, these are light gray and yellowish-gray medium- and coarse-grained massive, layered and unclearly banded rocks. In carbonate-silicate rocks, rounded grains of clinopyroxene and scapolite accumulations are clearly visible, and in silicate marbles, rounded grains of forsterite. In general, clinopyroxene-scapolite carbonate-silicate rocks predominate within the Khaptasynnakh formation, interbedded with clinopyroxene plagiogneisses.

Although these rocks have undergone granulite facies metamorphism, the primary structural and textural features of the sedimentary rocks are sometimes clearly visible. Sedimentary breccias are common at the base of the section, and, depending on the size of the detrital material, their appearance varies from “littered” marbles, often with acute-angled fragments of silicate rocks in a carbonate matrix, standing out in relief on the weathered surface, to coarse-grained breccias [13]. In addition to

This is an open access article under the CC BY 4.0 license

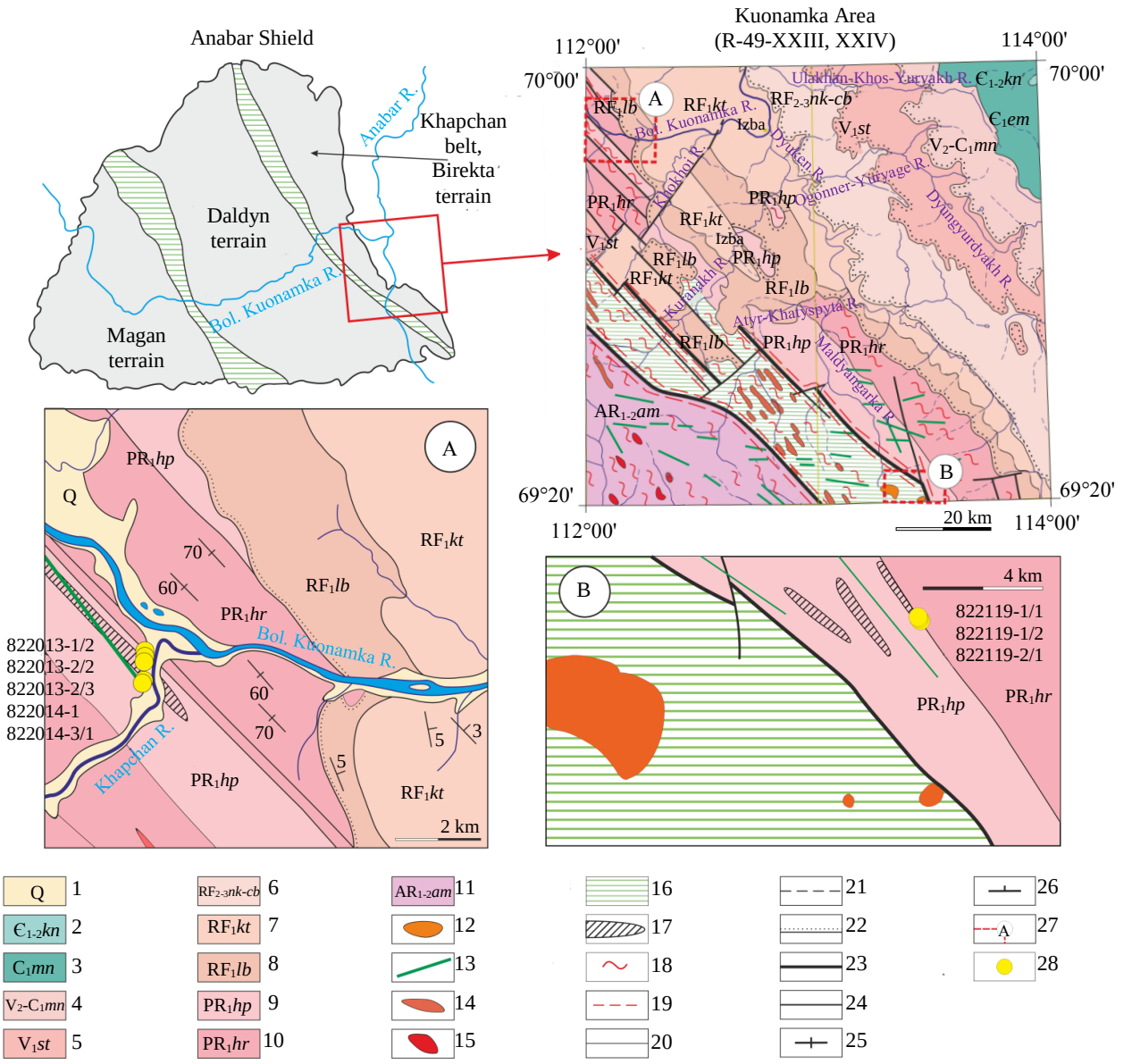


Fig.1. Sampling points in the inserts to the simplified geological map of sheet R-49-XXIII, XXIV (according to [9, 14], with changes)

1 – Quaternary deposits; 2 – Kuonamskaya suite; 3 – Emyaksinskaya suite; 4 – Manykayskaya suite; 5 – Starorechenskaya suite; 6 – Yusmactakhskaya suite; 7 – Kotuikanskaya suite; 8 – Labaztakhskaya suite; 9 – Khapchanskaya series; 10 – Khardakhskaya series; 11 – Ambardakhskaya strata; 12 – Kuonamsky kimberlite-carbonatite complex; 13 – Riphean dike complexes (qβRF1); 14 – Magan granites; 15 – Anabar granites; 16 – migmatite-gneiss complexes of melange zones; 17 – metacarbonate rocks; 18 – migmatized and granitized rocks; 19 – linear zones of tectonites; 20-22 – geological boundaries: conformable (reliable and inferred), unconformable; 23 – main faults; 24 – minor faults; 25 – linearity of rocks; 26 – bedding elements; 27 – boundaries of inserts; 28 – sampling points

sedimentary breccias, significantly more quartzose rock varieties are often observed at the base of the lenses. This may be due to higher concentrations of terrigenous material in the primary sediment.

In the course of the work, two lens-shaped bodies of metacarbonate rocks localized in the lower part of the Khapchan series section were studied (Fig.1). The northern lens (so-called 822013 and 822014) is located in the mouth of the Khapchan River (a tributary of the Bolshaya Kuonamka River) and was previously described in the explanatory note to the geological map R-49-XXIII, XXIV [14]. The lenticular member has a thickness of about 100 m and a length of 7 km; the rocks were identified as forsterite-diopside silicate marbles with a variable composition: calcite (30-85 %), diopside (5-50 %), forsterite (0-10 %), pargasite (5-10 %), phlogopite (5-10 %). The southern lens is located 80 km to the southwest and occupies a similar structural position in the section of the Khapchan series. The parameters (thickness and extent) of this lens are more difficult to determine due to poor exposure; in Fig.1 it is shown in accordance with the geological map R-49-XXIII, XXIV [14].

This is an open access article under the CC BY 4.0 license

Methods

Primary diagnostics of minerals in thin sections was carried out at the Research Center for X-ray Diffraction Research Methods at St. Petersburg State University using a Leica DM4500P polarizing microscope.

The chemical composition of rocks for major elements was determined by the XRF method on an ARL-9800 device, and for rare and rare earth elements – by the ICP-MS method on an ELAN-6100 DRC device in the central analytical laboratory of the Karpinsky Institute. To construct the REE distribution spectra, the composition of the rocks was normalized to PAAS [15].

The content of the major elements in minerals was determined using a Hitachi S-3400N scanning electron microscope with an AzTec Energy 350 energy-dispersive spectrometer and a set of standard samples at the Geomodel Research Center of St. Petersburg State University (analyst N.S.Vlasenko). The calculation of the crystal-chemical formulas of minerals based on microprobe analyses was performed using the Minal3 program (author D.V.Dolivo-Dobrovolskii), which implements well-known methods for calculating the crystal-chemical formulas of minerals [16]; the ACES-9 program [17] was used to calculate the crystal-chemical formulas of calcium amphibole. The symbols of the minerals are given according to [18].

The content of rare earth and trace elements in minerals was measured in the same areas (crater diameter of about 20 μm) as the oxides of the main elements, using a Cameca IMS-4f ion microprobe at the Yaroslavl Branch of the Institute of Physics and Technology (analysts S.G.Simakin, E.V.Potapov) using a standard technique. Survey conditions: a primary beam of $^{16}O_2^-$ ions with a diameter of about 15-20 μm was used; ion current was 5-7 nA; accelerating voltage of the primary beam was 15 keV. Each measurement consisted of three cycles, which made it possible to estimate the reproducibility of the measurement results. The total analysis time for one point averaged 30 min. The size of the studied mineral area did not exceed 15-20 μm in diameter; the relative measurement error for most elements was 10-15 %; the element detection threshold was, on average, 10 ppb. When constructing the REE distribution spectra, their composition was normalized to the composition of the CI chondrite [19].

Physicochemical analysis of parageneses was carried out using the Perple_X software package (Perple_X version 6.9.0) [20]. The petrochemical data used for the calculation (see Table) were pre-calculated for dry weight; MnO, P_2O_5 and part of CaO corresponding to apatite were subtracted from the composition to simplify the calculation; Fe_2O_3, if present in the composition, was recalculated to FeO. The thermodynamic database of minerals and fluids hp02ver.dat [21, 22] was used in all calculations. The following solid solution models were selected (solution_model.dat file): for monoclinic amphibole – Amph(DPW), for orthorhombic amphibole – o-Amph, for garnet – Gt(HP), for staurolite – St(HP), for biotite – Bio(HP), for feldspars – feldspar, for spinel – Sp(HP), for orthopyroxene – Opx(HP), for clinopyroxene – Cpx(HP), for cordierite – hCrd, for muscovite – Mica(M), for chlorite – Chl(HP), for carbonates – Do(HP) and M(HP), for melt – melt(HP) (URL: http://www.perplex.ethz.ch/).

Chemical composition of metacarbonate rocks of the Khapchan series

Elements	Rocks									Lower limits
	Silicate marbles					Carbonate-silicate rocks				
	822013-1/2	822013-2/2	822013-2/3	822014-1	822014-3/1	822119-1/1	822119-1/2	822119-2/1	822119-2/2	
SiO_2, %	14.5	15.5	17.9	23.9	6.21	64.6	64.9	34.8	–	0.02
TiO_2, %	0.091	0.09	0.07	0.15	0.075	0.51	0.62	0.24	–	0.01
Al_2O_3, %	2.27	3.25	2.95	3.92	1.91	14.2	15.1	7.52	–	0.05
Fe_2O_3, %	0.49	0.62	0.59	0.71	0.61	0.67	0.85	0.84	–	0.3
FeO, %	0.86	0.61	0.48	1.08	0.48	3.15	2.65	1.69	–	0.25
MnO, %	0.036	0.028	0.027	0.097	0.019	0.074	0.06	0.033	–	0.01
MgO, %	10.6	12.1	11.5	15.5	11.4	1.36	1.01	1.27	–	0.1
CaO, %	38.8	36.7	36.7	27.4	40.9	9.54	8.48	30.5	–	0.01
Na_2O, %	<0.1	<0.1	<0.1	0.16	<0.1	1.57	1.81	1.27	–	0.1
K_2O, %	0.52	1	1.37	0.5	0.16	2.91	2.86	2.11	–	0.01
P_2O_5, %	0.067	0.098	0.099	0.21	<0.05	0.1	0.15	0.13	–	0.05
LOI, %	31.4	29.9	28.2	26.2	38.2	0.6	0.93	19.1	–	0.1
Total	99.9	99.9	99.9	100	100	99.6	99.6	99.7	–	–
Ba, %	0.0066	0.011	0.012	0.016	0.0054	0.11	0.096	0.09	–	0.005

This is an open access article under the CC BY 4.0 license

End of Table

Elements	Rocks									Lower limits
	Silicate marbles					Carbonate-silicate rocks				
	822013-1/2	822013-2/2	822013-2/3	822014-1	822014-3/1	822119-1/1	822119-1/2	822119-2/1	822119-2/2	
Li, ppm	5.6	5.6	7.28	7.94	1.13	8.86	8.33	5.82	5.34	1
Sc, ppm	2.88	2.64	2.17	4.26	2.5	9.87	12.2	6.5	6.58	0.2
Co, ppm	1.78	1.74	1.16	3.77	0.89	8.06	7.9	5.22	5.65	0.5
Ni, ppm	3.54	3.31	2.25	6.32	1.75	11	10.8	13.2	13	1
Cu, ppm	3.86	2.53	1.41	2.46	<1	14.8	15.3	11.4	14.4	1
Zn, ppm	10.4	11.2	17.3	14.7	1.71	90.6	91.1	50.2	38.9	1
Ge, ppm	0.4	0.29	0.34	0.35	0.13	1.31	1.56	0.88	0.86	0.1
Ag, ppm	0.021	0.017	0.017	0.087	0.012	0.11	0.14	0.078	0.083	0.01
Sb, ppm	<0.1	<0.1	<0.1	0.36	0.14	<0.1	<0.1	<0.1	<0.1	0.1
Tl, ppm	0.16	0.3	0.52	<0.1	<0.1	0.43	0.44	0.33	0.35	0.1
Pb, ppm	4.4	3.83	6.39	5.87	1.76	22.1	24.1	20.6	22.8	1
As, ppm	<0.5	<0.5	<0.5	<0.5	<0.5	1.48	2.25	3.25	2.85	0.5
Be, ppm	<1	<1	1.26	1.2	<1	2.98	2.97	1.81	1.98	1
V, ppm	11.4	13.1	14.4	29.2	9.78	49.6	69.9	34.9	38.9	2.5
Cr, ppm	7.96	5.44	7.53	12.9	2.79	22.9	28.1	32.8	33.5	1.0
Rb, ppm	29.1	64.2	81.6	11.5	<2	93.2	89.2	61.3	65.1	2
Sr, ppm	396	396	328	335	189	1970	2140	4850	1860	1
Y, ppm	10.4	5.39	6.55	8.45	3.08	28.7	37.6	18.1	18.8	0.1
Zr, ppm	35.6	29.6	39.8	156	42.4	202	211	141	161	0.5
Nb, ppm	3.78	4.65	5.48	4.5	<0.5	22.2	25	11	11.1	0.5
Mo, ppm	0.66	0.65	30.2	0.68	<0.6	5.81	9.12	3.01	1.81	0.6
Sn, ppm	14.4	1.25	1.19	0.91	<0.2	2.76	3.14	1.53	1.2	0.2
La, ppm	19	12.6	17.7	9.63	4.75	49.1	68.5	79	69.9	0.01
Ce, ppm	40.2	25.6	33.3	20.9	9.55	97.3	136	140	129	0.01
Pr, ppm	4.56	2.81	3.29	2.47	1.16	11.6	16.5	15	14	0.01
Nd, ppm	16.1	9.68	11.1	8.84	4.45	40.5	57.1	48.3	47.4	0.01
Sm, ppm	3.07	1.94	2.07	1.51	0.88	8.74	13.1	7.6	7.06	0.005
Eu, ppm	0.26	0.3	0.23	0.42	0.15	1.8	2.08	1.49	1.48	0.005
Gd, ppm	2.56	1.51	1.67	1.39	0.62	6.28	8.78	5.57	5.43	0.01
Tb, ppm	0.3	0.17	0.21	0.22	0.089	0.9	1.35	0.79	0.64	–
Dy, ppm	1.66	0.86	1	1.23	0.51	5.39	6.87	3.63	3.27	–
Ho, ppm	0.29	0.14	0.16	0.26	0.098	0.97	1.36	0.64	0.59	–
Er, ppm	0.84	0.48	0.55	0.84	0.25	3	3.95	1.79	1.76	–
Tm, ppm	0.14	0.074	0.085	0.12	0.042	0.48	0.62	0.3	0.27	–
Yb, ppm	0.93	0.41	0.55	0.8	0.24	2.82	3.9	1.67	1.63	–
Lu, ppm	0.15	0.062	0.068	0.13	0.028	0.45	0.58	0.27	0.29	–
Ta, ppm	1	0.87	1.12	2.67	0.93	5.3	5.74	3.55	0.81	–
W, ppm	<0.5	<0.5	2.51	3.56	0.68	2.88	2.93	0.99	0.74	–
Th, ppm	4.21	4.4	7.4	1.46	0.12	10.9	15.4	16	15.3	–
U, ppm	2.07	2.16	2.95	1.6	<0.1	4.6	6.37	4.38	3.89	–

Petrography

According to the current classification of metacarbonate rocks [23], the rocks in question can be divided into two groups based on their mineral composition: silicate marbles (carbonate content 95-50 %) and carbonate-silicate rocks (carbonate mineral content 5-50 %). Silicate marbles are distributed

This is an open access article under the CC BY 4.0 license

within the lenticular body in the northwest of the territory under discussion (Fig.1, A, samples 822013, 822014), and carbonate-silicate rocks are found in the southeast (Fig.1, B, samples 822119).

The matrix of fine- to medium-grained silicate marbles is composed of calcite (80-90 %), with a small amount of dolomite (up to 10 %). It contains rounded porphyroblasts of forsterite (5-15 %) and clinopyroxene (up to 20 %), less often spinel (up to 5 %) and calcium amphibole (up to 5 %); sometimes there are phlogopite leaflets (up to 5 %), plagioclase, potassium feldspar (single grains), clinohumite (up to 15 %). Accessory minerals are represented by apatite, zircon, barite, fluorite, magnetite, molybdenite, and pyrite. Secondary minerals are represented by serpentine, developing after forsterite and minerals of the humite group, and chlorite, developing after clinopyroxene. Relicts of orthopyroxene, intensively replaced by clinopyroxene and calcite, are very rare. Clinopyroxene rims are also noted around forsterite (Fig.2, *a*, *b*). Grains of potassium feldspar are surrounded by complex zonal rims, in the inner parts of which thin clinopyroxene-plagioclase symplectites are widespread, and the outer part is composed of phlogopite (Fig.2, *c, d*). Dolomite rims are sometimes observed around spinel. Clinohumite is distributed unevenly in the rocks (found in samples 822013-2/2, 822014-1), apparently in spots: in those areas where clinohumite porphyroblasts appear, there is significantly less clinopyroxene and forsterite, but clinohumite itself is often closely spatially associated with clinopyroxene, probably replacing it (Fig.2, *e*, *f*). There are small quartz veinlets up to 1 cm thick, which are surrounded by clusters of clinopyroxene, feldspars (both plagioclase and potassium feldspar), and phlogopite. Plagioclase within such veinlets is often surrounded by a rim of scapolite (Fig.2, *g*, *h*). Thus, spinel and forsterite are found in association with quartz within the thin section, but are not in direct contact with it. The most intensive replacement of forsterite by clinopyroxene is noted precisely near these veinlets. In the marginal parts of the body of silicate marbles, the number of such quartz veins increases, and areas of clinopyroxene-two-feldspar composition appear, in which carbonates disappear (sample 822013-2/3).

In fine- to medium-grained carbonate-silicate rocks, the matrix is composed of calcite (35-45 %) and quartz (30-35 %), less often plagioclase and potassium feldspar (up to 5 %), which are sometimes distributed evenly, sometimes unevenly, in spots; quartz is often concentrated in the form of clusters of small grains around large grains of potassium feldspar, in which perthites are often observed. The matrix of the rock contains rounded clinopyroxene porphyroblasts up to 2-3 mm in size (5-10 %), smaller rounded or elongated garnet grains (about 10 %). Scapolite and plagioclase are found in subordinate quantities. Accessory minerals are represented by titanite, zircon, magnetite, pyrite, and apatite. There are isolated small rounded grains of vesuvianite, in which the analyzer shows a pronounced oscillatory zoning. Feldspars are intensively pelitized, plagioclase is sericitized.

Rock composition

The rocks we studied show wide variations in chemical composition, expressed in an increase in the content of SiO_2, Al_2O_3, Na_2O, and K_2O as the content of CaO and MgO decreases (see Table). Silicate marbles contain 6.21-23.9 wt.% SiO_2, carbonate-silicate rocks contain 34.8-64.9 wt.% SiO_2. Within each of the studied metacarbonate rock bodies, a clear zoning of silica content in the rocks is observed: samples taken from the central part are less rich in SiO_2, FeO than samples confined to the periphery of metacarbonate rock bodies, but are enriched in MgO, CaO. A detailed study of the distribution spectra of REE and rare elements in silicate marbles and carbonate-silicate rocks of the Khapchan series is given in the work [24], we will note only some features.All the studied rocks are characterized by a relatively flat REE distribution spectrum (Fig.3), the total content of which in carbonate-silicate rocks is an order of magnitude higher than in silicate marbles: in silicate marbles ∑REE from 22.8 to 90.1 ppm, while in carbonate-silicate rocks ∑REE from 229 to 321 ppm. Almost all samples show enrichment of LREE with respect to HREE (La/Yb 21.5 on average, La/Sm 5.9 on average). Some of the REE distribution spectra in silicate marbles are characterized by a pronounced negative Eu anomaly (Fig.3), which is generally typical of carbonate-silicate rocks [25], but sometimes a positive Eu anomaly is also noted. At the same time, carbonate-silicate rocks are more likely to be characterized by a small positive Eu anomaly.

This is an open access article under the CC BY 4.0 license

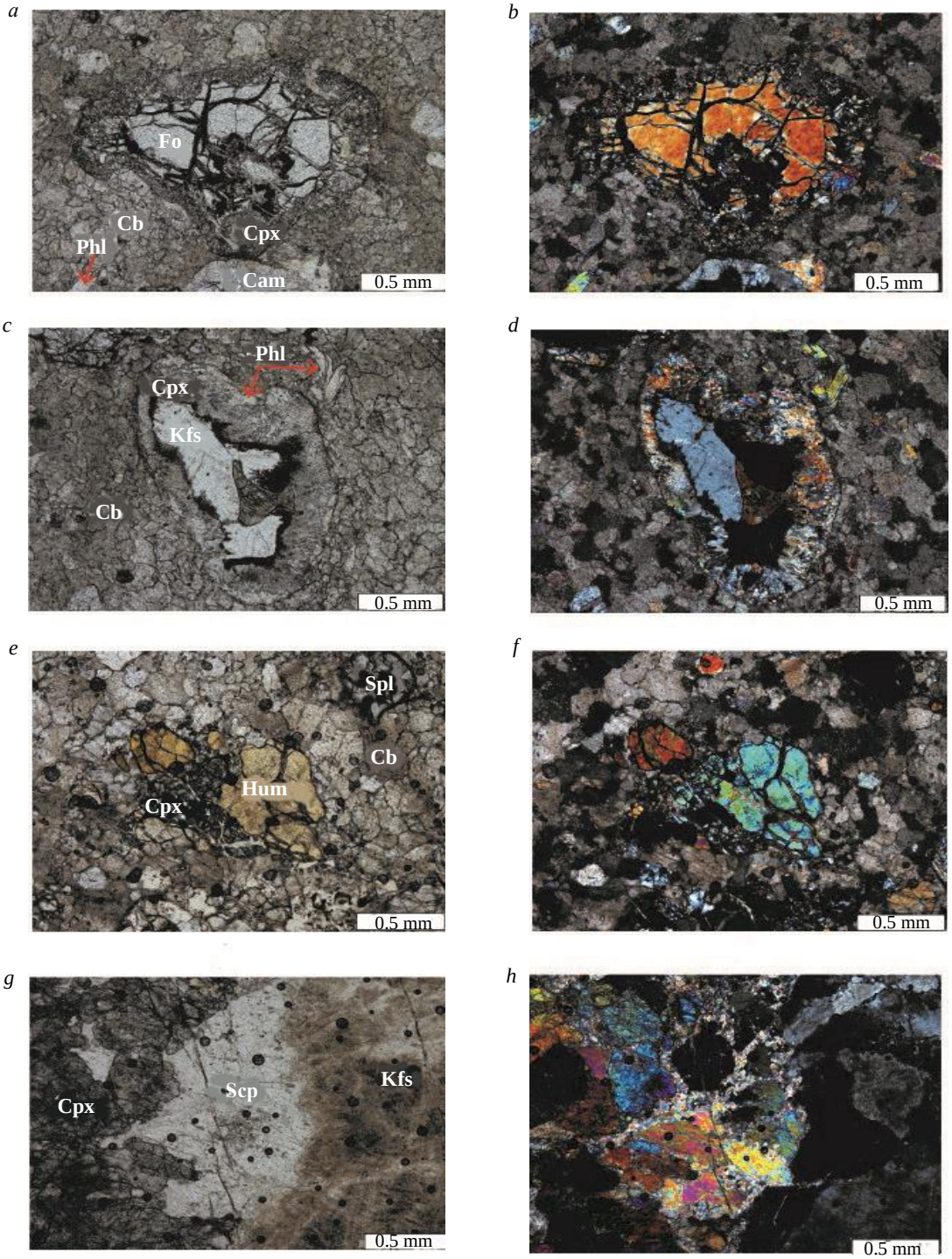


Fig.2. Photographs of thin sections of silicate marbles, on the left – without an analyzer, on the right – with an analyzer: *a*, *b* – replacement of forsterite by diopside at the contact with calcite; *c*, *d* – replacement of potassium feldspar by clinopyroxene and phlogopite at the contact with calcite; *e*, *f* – clinohumite and diopside; *g*, *h* – development of secondary meionite around potassium feldspar
The symbols of minerals in the photo are given according to [18]

The content of a number of minor and rare elements (Cr, Co, V) in carbonate-silicate rocks correlates relatively well with SiO_2 and Al_2O_3. This is probably due to the fact that these rare elements were present in the composition of the terrigenous admixture in the protolith of carbonate-silicate rocks. Wide variations in the content of U (<0.1-6.4 ppm) and Th (0.12-16 ppm) are observed, the Th/U ratio varies from 0.9 to 3.9 ppm, although Th/U ≤ 2 is usually characteristic of "pure" carbonate rocks [1]. In this case, wide variations in the content of U and Th may indicate the presence of these trace elements in the composition of the varying silicate admixture.

This is an open access article under the CC BY 4.0 license

© Ekaterina Yu. Akimova, Nikolai I. Gusev, Aleksandr D. Savelev, Daniil R. Donchenko, 2025

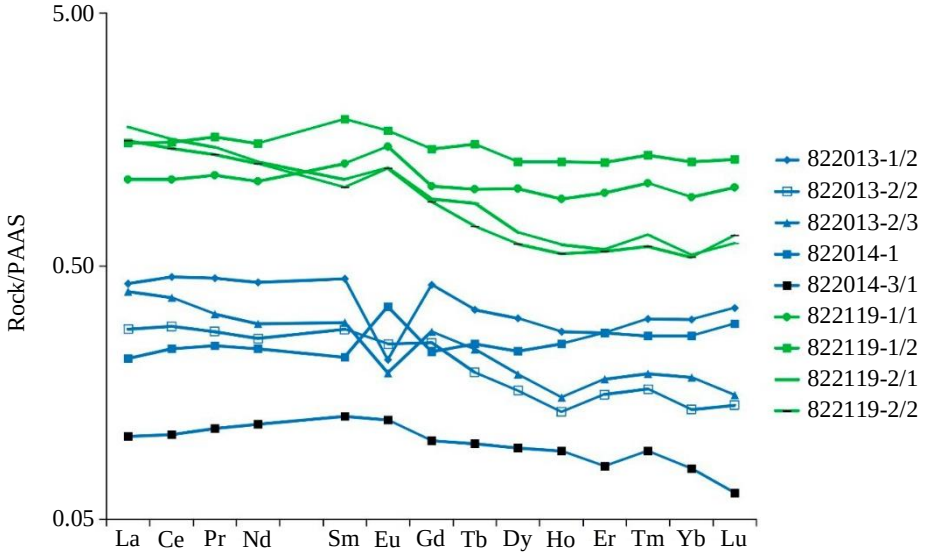


Fig.3. Distribution of rare earth element contents in silicate marbles (shown in blue) and carbonate-silicate rocks (shown in green)

Composition of minerals

Major elements. *Carbonates* in silicate marbles are represented by calcite and dolomite (Fig.4, *a*). Calcite sometimes contains admixtures of Mg up to 0.20 formula coefficients (f.c.), Si up to 0.09 f.c., Fe^{2+} up to 0.01 f.c. Dolomite always contains admixtures of Fe up to 0.03 f.c., sometimes contains admixtures of Si up to 0.09 f.c., rarely – admixtures of Mn up to 0.03 f.c. In carbonate-silicate rocks, carbonates are represented exclusively by calcite, rarely it contains admixtures of Mg, Fe^{2+} up to 0.01 f.c.

Pyroxenes (according to classification [26]) are represented by enstatite (found only in silicate marbles) and diopside (Fig.4, *b*). Enstatite apparently does not contain Fe^{2+}, since the amount of Mg in it is constantly about 2 f.c., while Fe^{3+} is present in the Si position – the content of calculated Fe^{3+} is up to 0.16 f.c. Al admixture is less common – up to 0.02 f.c. A slight admixture of Ca is characteristic up to 0.03 f.c. Ferrous diopside – *x*Mg from 0.79 to 0.99, constantly contains Al admixture – up to 0.16 f.c., sometimes contains Ti admixtures up to 0.03 f.c., Fe^{3+} up to 0.02 f.c., Na up to 0.04 f.c. In carbonate-silicate rocks, diopside is significantly more ferrous – *x*Mg from 0.51 to 0.77, often contains impurities of Al and Na up to 0.05 f.c., sometimes impurities of Fe^{3+} and Mn up to 0.01 f.c.

Feldspars are represented by potassium feldspar (orthoclase, microcline) and plagioclase (Fig.4, *c*). In silicate marbles, plagioclase occurs only as perthites in potassium feldspar, where it is represented by almost pure albite, in clinopyroxene-plagioclase symplectites around potassium feldspar, where it is represented by albite-oligoclase (An from 10 to 22), and in the rims of quartz veins, where it is represented by andesine (An from 30 to 36). Potassium feldspar constantly contains an admixture of Ba up to 0.12 f.c., Na up to 0.21 f.c. In carbonate-silicate rocks, plagioclase is represented by oligoclase An from 13 to 19, potassium feldspar constantly contains impurities of Ba up to 0.02 f.c., Na up to 0.11 f.c., and sometimes contains an impurity of Sr up to 0.02 f.c.

Phlogopite (according to classification [27]) is found only in silicate marbles; its composition differs in varieties with and without clinohumite (Fig.4, *d*). In varieties without clinohumite, phlogopite contains a constant admixture of Ti up to 0.05 f.c., Fe^{2+} up to 0.08 f.c., F 0.47-0.96 f.c., sometimes Fe^{3+} up to 0.09 f.c., Ca up to 0.20 f.c., Na up to 0.07 f.c.; the ^{D}Al content varies from 0.03 to 0.17 f.c. In varieties with clinohumite, it contains a constant admixture of F 1.01-1.47 f.c., i.e. it is fluorophlogopite. Does not contain calculated Fe^{2+}, constantly contains Fe^{3+} impurity up to 0.08 f.c., Ba up to 0.11 f.c., Na up to 0.11 f.c.; ^{D}Al is present inconstantly up to 0.10 f.c. Rare impurities of Ti up to 0.03 f.c., Ca up to 0.14 f.c., Cl up to 0.02 f.c.

Calcium amphibole is also found only in silicate marbles, forming the pargasite-fluoropargasite series (according to the classification [28]): ^{B}Ca/^{B}(Ca+Na) on average 0.99, ^{C}(Al+Fe^{3+}+2Ti) on average 0.91 f.c., ^{A}(Na+K+2Ca) on average 0.96 f.c. (Fig.4, *e*) (distribution of cations by positions and classification in accordance with [28]). The content of ^{T}Al is from 1.42 to 1.91 f.c., ^{C}Al from 0.56 to

This is an open access article under the CC BY 4.0 license

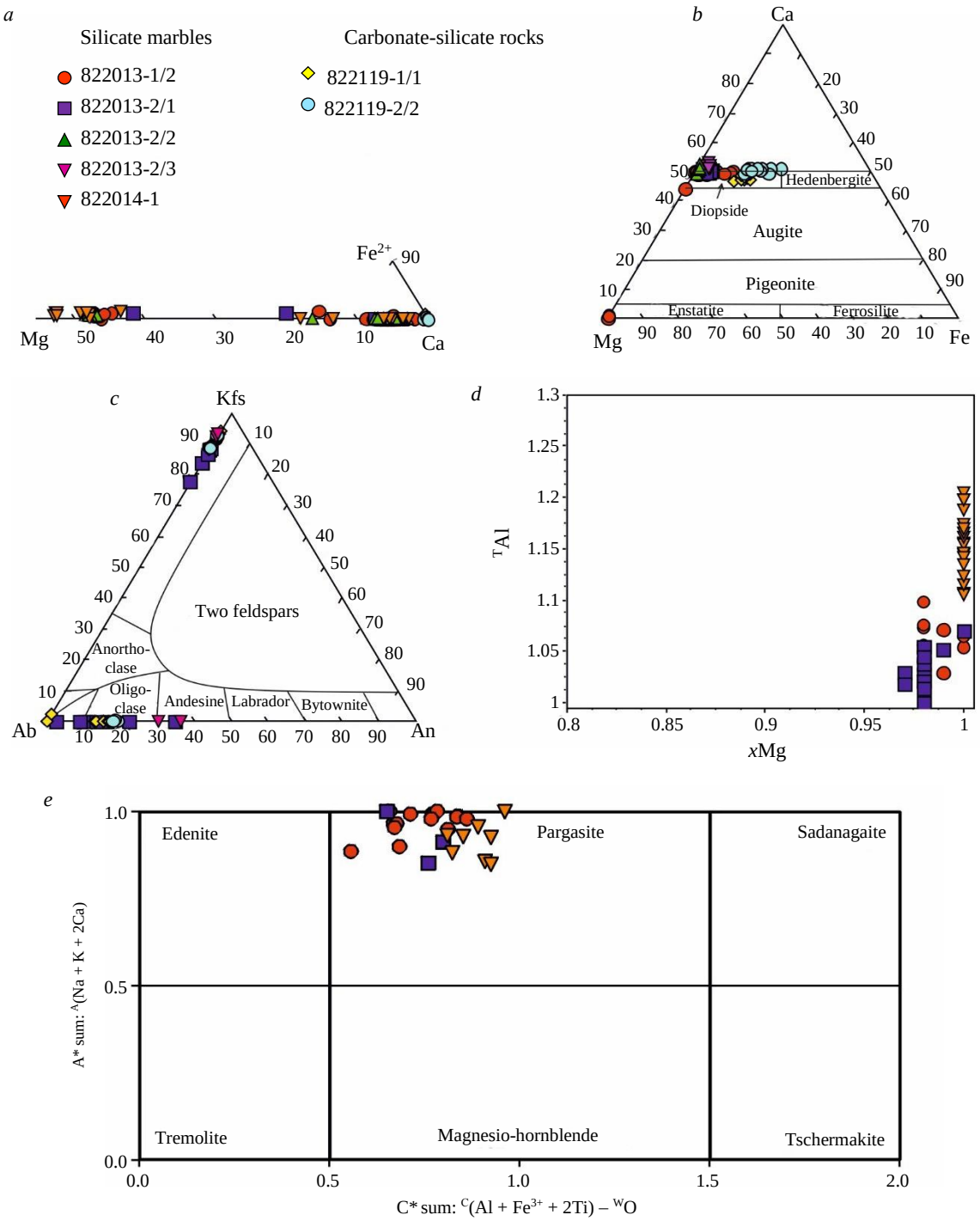


Fig.4. Diagrams of mineral compositions: *a* – carbonates; *b* – pyroxenes; *c* – feldspars; *d* – phlogopite; *e* – calcium amphibole [28]

0.78 f.c., ^{C}Mg from 3.96 to 4.32 f.c. The constant presence of F in the W position is characteristic: from 0.70 to 1.32 f.c. In calcium amphiboles from silicate marbles with clinohumite, an admixture of Cl up to 0.03 f.c. is sometimes also noted.

Forsterite is found only in silicate marbles, the Fe^{2+} content is up to 0.13 f.c., sometimes there is an admixture of Mn up to 0.01 f.c., rarely – Cl up to 0.01 f.c.

Garnet is found only in carbonate-silicate rocks, where it is represented by grossular (according to classification [29]), the Fe^{2+} content is up to 0.52 f.c., often contains impurities of Ti up to 0.07 f.c., Fe^{3+} up to 0.69 f.c., sometimes Mn up to 0.02 f.c.

Scapolite in silicate marbles is represented by meionite containing Na up to 1.29 f.c., K up to 0.05 f.c., Cl up to 0.15 f.c. In carbonate-silicate rocks, scapolite is represented by marialite containing Ca up to 1.43 f.c., K up to 0.13 f.c., Cl up to 0.55 f.c.

This is an open access article under the CC BY 4.0 license

Vesuvianite is found only in carbonate-silicate rocks, the calculated content of Fe^{3+} is up to 1.73 f.c., Ti up to 1.14 f.c.; it constantly contains F up to 3.79 f.c. and Cl up to 0.59 f.c., rarely S up to 0.25 f.c.

Clinohumite is found only in silicate marbles, contains Fe^{2+} up to 0.35 f.c., Ti up to 0.10 f.c., sometimes Fe^{3+} up to 0.21 f.c.

Spinel (according to the classification [30]) is pure spinel, found only in silicate marbles, xFe^{2+} up to 0.12 f.c., xFe^{3+} up to 0.04 f.c., Zn impurity is rarely found up to 0.08 f.c.

Titanite usually contains F up to 0.28 f.c., Fe^{3+} up to 0.04 f.c.

Apatite in all varieties of the studied rocks is represented by fluorapatite, sometimes containing an admixture of Si up to 0.07 f.c., Cl up to 0.06 f.c.

Rare earth and trace elements. *Clinopyroxene.* The content of rare earth elements in clinopyroxene was analyzed both in silicate marbles (3 points) (Fig.5, *b*) and in carbonate-silicate rocks (2 points) (Fig.6, *b*). Clinopyroxene from silicate marbles is characterized by a relatively low total REE content from 1.52 to 5.19 ppm, with the lowest total REE content characteristic of clinopyroxene present in the form of rims around forsterite (analysis 10). Clinopyroxene developed after forsterite is depleted (relative to clinopyroxene from the matrix of silicate marbles) in the entire REE spectrum by approximately an order of magnitude. The REE distribution spectrum in this clinopyroxene is rather flat, without Eu-anomaly, while clinopyroxene from the matrix of silicate marbles is distinguished by a slightly convex spectrum in the LREE region with a small negative Eu-anomaly (Eu/Eu* from 0.35 to 0.20). The Ti content in clinopyroxene from the matrix of silicate marbles is quite high – from 737 to 1304 ppm, while in clinopyroxene developing after forsterite the Ti content is significantly lower – 357 ppm. Clinopyroxene from carbonate-silicate rocks is characterized by a slightly higher total REE content (from 7.40 to 14.8 ppm) and a different, sinusoidal REE distribution spectrum, convex in the LREE region (total LREE content from 6.49 to 11.6 ppm) and concave in the HREE region (total HREE content from 0.52 to 2.47 ppm). It is also characterized by a small negative Eu anomaly (Eu/Eu* from 0.55 to 0.23). The Ti content is relatively low – from 184 to 259 ppm.

Feldspars. The rare earth element content was analyzed in potassium feldspar from silicate marbles (2 points) (see Fig.5, *c*), as well as in potassium feldspar (1 point) (Fig.6, *d*) and plagioclase (2 points) from carbonate-silicate rocks (Fig.6, *c*). All analyzed potassium feldspars are characterized by a relatively constant, low total REE content from 6.98 to 9.62 ppm, a well-defined positive Eu anomaly (Eu/Eu* from 121 in potassium feldspar from silicate marbles to 359 in potassium feldspar from carbonate-silicate rocks). Potassium feldspar from silicate marbles is significantly depleted in LREE, except for La (total LREE content is from 1.65 to 1.77 ppm), in potassium feldspar from carbonate-silicate rocks the total LREE content is slightly higher – 2.11 ppm. All analyzed potassium feldspars are characterized by high contents, ppm: Rb – 265-276 in silicate marbles and 427 in carbonate-silicate rocks; Sr – 1,117-1,711 and 2,669; Ba – 12,454-14,028 and 7,870 respectively. Plagioclase from carbonate-silicate rocks is characterized by a low total REE content from 0.57 to 2.51 ppm without a pronounced Eu anomaly (Eu/Eu* is 0.80 and 1.78). Contains a significant amount of Sr up to 3,499 ppm.

Phlogopite. The rare earth element content was analyzed in phlogopite from the matrix of silicate marbles (1 point) and in phlogopite developing around potassium feldspar (1 point) (see Fig.5, *c*). Both REE distribution spectra were found to be virtually identical; in terms of shape in the LREE region, they largely repeat the shape of the REE distribution spectrum in potassium feldspar, which suggests that phlogopite inherited the REE distribution spectrum of potassium feldspar, along which it developed. At the same time, phlogopite contains an order of magnitude less HREE than the potassium feldspar it replaces: the total HREE content in phlogopite is about 0.42 ppm, versus 2.59-2.96 in potassium feldspar. It should be noted that phlogopite also has an increased content of Rb up to 258 ppm, Ba up to 1,707 ppm, while the Ti content in it is much higher (1,512-2,851 ppm versus 194-278 ppm in potassium feldspar).

This is an open access article under the CC BY 4.0 license

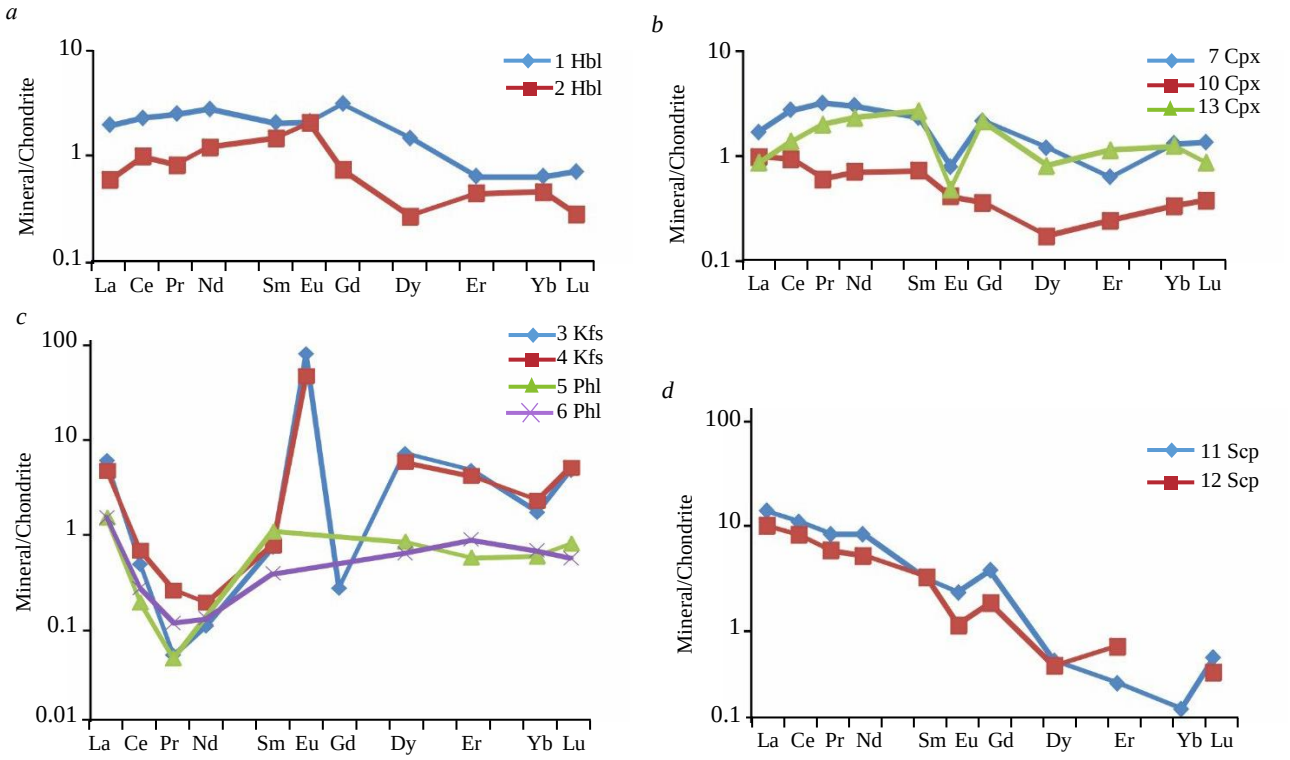


Fig.5. REE distribution spectra in minerals of silicate marbles (sample 822013-1/2):
a – in calcium amphibole; *b* – in clinopyroxene; *c* – in potassium feldspar and phlogopite; *d* – in scapolite

Forsterite. The content of rare earth elements in forsterite from silicate marbles was analyzed at 2 points, it turned out to be extremely low (total LREE content – from 0.11 to 0.16 ppm, HREE content below the detection threshold), a fairly high Cr content is noteworthy up to 410 ppm, an admixture of Mn is present up to 323 ppm.

Calcium amphibole from silicate marbles was analyzed at 2 points (see Fig.5, *a*), it is characterized by a low total REE content from 2.06 to 4.93 ppm and a flat REE distribution spectrum without Eu anomalies. The Ti content is about 2,250 ppm, and a slightly elevated Nb content is characteristic up to 25.5 ppm.

Garnet from carbonate-silicate rocks was analyzed at three points (Fig.6, *a*). The total REE content in it is from 101 to 138 ppm, the LREE/HREE ratio varies from 0.09 to 0.18. The garnet is characterized by a smooth REE distribution spectrum, with a slight positive slope in the LREE region and gradually flattening out in the HREE region (Lu_N/Gd_N from 1.18 to 2.10). A small negative Eu anomaly is noted: Eu/Eu* is about 0.82. The REE distribution spectra of the analyzed garnets show similarity with the spectra of garnets from carbonate-silicate rocks of the Kusinsko-Kopansky complex in the Southern Urals [5]. Characterized by high content, ppm: Ti 2,878-3,929, V up to 319, Cr up to 216, Mn up to 2,006, Y up to 251.

Scapolite. The rare earth element content was analyzed both in meionite from silicate marbles (2 points) (see Fig.5, *d*) and in marialite from carbonate-silicate rocks (2 points) (Fig.6, *d*). Meionite from silicate marbles is characterized by a low total REE content 11.4-16.0 ppm, a smooth spectrum with a noticeable negative slope (the LREE/HREE ratio varies from 15.1 to 17.4), and a small negative Eu anomaly Eu/Eu* 0.44-0.67. An elevated Sr content is noted – 985-1,099 ppm. Marialite from carbonate-silicate rocks is characterized by an even lower total REE content 6.42-7.97 ppm, a flat REE distribution spectrum (the LREE/HREE ratio varies from 1.66 to 3.55) with a positive Eu anomaly Eu/Eu* from 1.46 to 18.9. It should be noted that the REE distribution spectra in marialite from carbonate-silicate rocks to a significant extent, especially in the HREE region, repeat the shape of the REE distribution spectra in potassium feldspar. Marialite probably inherited the REE distribution

This is an open access article under the CC BY 4.0 license

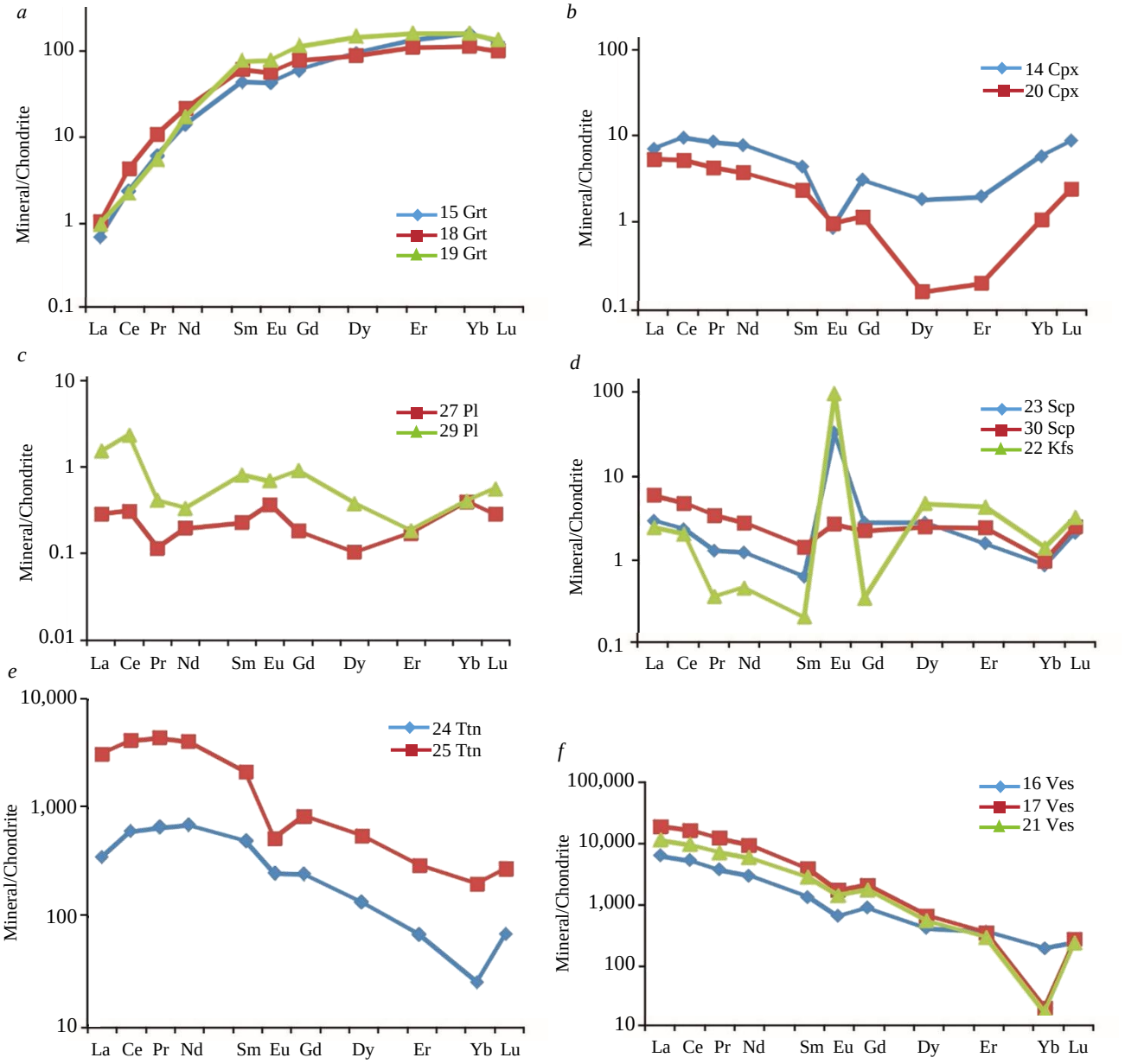


Fig.6. REE distribution spectra in minerals of carbonate-silicate rocks (sample 822119-1/1):
a – in garnet; *b* – in clinopyroxene; *c* – in plagioclase; *d* – in scapolite; *e* – in titanite; *f* – in vesuvianite

spectrum of potassium feldspar, along which it developed. At the same time, marialite contains an order of magnitude more LREE than the potassium feldspar it replaces: in marialite, the total LREE content is up to 5.94 ppm, while in potassium feldspar it is 2.11 ppm. As in meionite from silicate marbles, in marialite from carbonate-silicate rocks, an increased Sr content is recorded – 1,390-2,204 ppm. In addition, the latter also has an increased Ba content – 3,640-5,031 ppm. Probably, these features of the rare-element composition are also inherited by marialite from potassium feldspar.

Vesuvianite from carbonate-silicate rocks was analyzed at 3 points (Fig.6, *f*). Points 16 and 17 are located, respectively, in the center and at the edge of one large zonal grain. The total REE content differs significantly in the central (6,970 ppm) and edge (21,080 ppm) parts of the grain, and this difference is recorded for both LREE (from 6368 ppm in the center to 19,779 ppm at the edge) and HREE (from 370 ppm in the center to 638 ppm at the edge). All analyzed vesuvianites are characterized by a smooth REE distribution spectrum with a pronounced negative slope (the LREE/HREE ratio varies from 17.3 to 31.0), a small negative Eu anomaly Eu/Eu* about 0.60. Vesuvianite is characterized by a high Ti content up to 23,888 ppm, increased Mn content up to 605 ppm, Sr up to 906 ppm.

This is an open access article under the CC BY 4.0 license

Titanite from carbonate-silicate rocks was analyzed at two points (Fig.6, *e*) within one large grain that was heterogeneous in optics. These two areas of one grain showed a difference in the total REE content from 1,034 to 6,344 ppm, while the REE distribution spectrum in shape was the same in them: with a pronounced negative slope, convex in the LREE area, with a small negative Eu anomaly Eu/Eu* 0.35-0.68. An increased content of a number of rare elements was noted – V up to 1,101 ppm, Zr up to 2,089 ppm, Nb up to 1,728 ppm, Y up to 536 ppm. Further study of this mineral is required to understand what causes the variations in its composition within the grain.

Thermodynamic modeling

It is assumed that the rocks of the Khapchan series (sillimanite-cordierite-biotite-garnet, sillimanite-biotite-garnet, garnet-biotite gneisses and garnet-orthopyroxene gneisses with potassium feldspar) were metamorphised under granulite facies metamorphism conditions with a subsequent decrease in temperature to amphibolite facies conditions [11, 13]. However, no reconstruction of *PT*-metamorphic conditions for the metacarbonate rocks studied by us or other rockswithin the Khapchan series, has been previously performed due to the impossibility of obtaining *PT*-estimates for metacarbonate rocks using classical thermobarometry methods.

Construction and analysis of pseudosections is the most optimal method for reconstructing *PT*-conditions of carbonate rocks metamorphism. Phase equilibrium diagrams with stability fields of equilibrium mineral associations in *P–T* coordinates (pseudosections) are constructed for a given chemical composition of representative samples of silicate marbles and carbonate-silicate rocks in the SiO_2-TiO_2-Al_2O_3-FeO-MgO-CaO-Na_2O-K_2O-CO_2-H_2O system. To simulate the conditions of participation of essentially carbon dioxide fluid with a small proportion of water in mineral formation, $X(CO_2) = 0.9$ was specified.

Considering the close spatial arrangement and similar structural position of the studied carbonate-silicate rocks and silicate marbles, we assumed that we would obtain similar PT-conditions of metamorphism for these two varieties [31]. However, the obtained diagrams show how significantly the *PT*-conditions of stability of the studied parageneses differ.

In the pseudosection for the given composition of silicate marbles (sample 822013-1/2, Fig.7, *a*), the observed paragenesis Ol + Cpx + Cam + Bt + Cal + Spl occupies the region of moderate pressures (up to approximately 8 kbar) and high temperatures (approximately 700-900 °C). A slight decrease in temperature leads to the replacement of spinel by dolomite, which is observed in thin sections. The upper limit of the stability of the observed paragenesis by pressure is limited by associations without calcium amphibole.

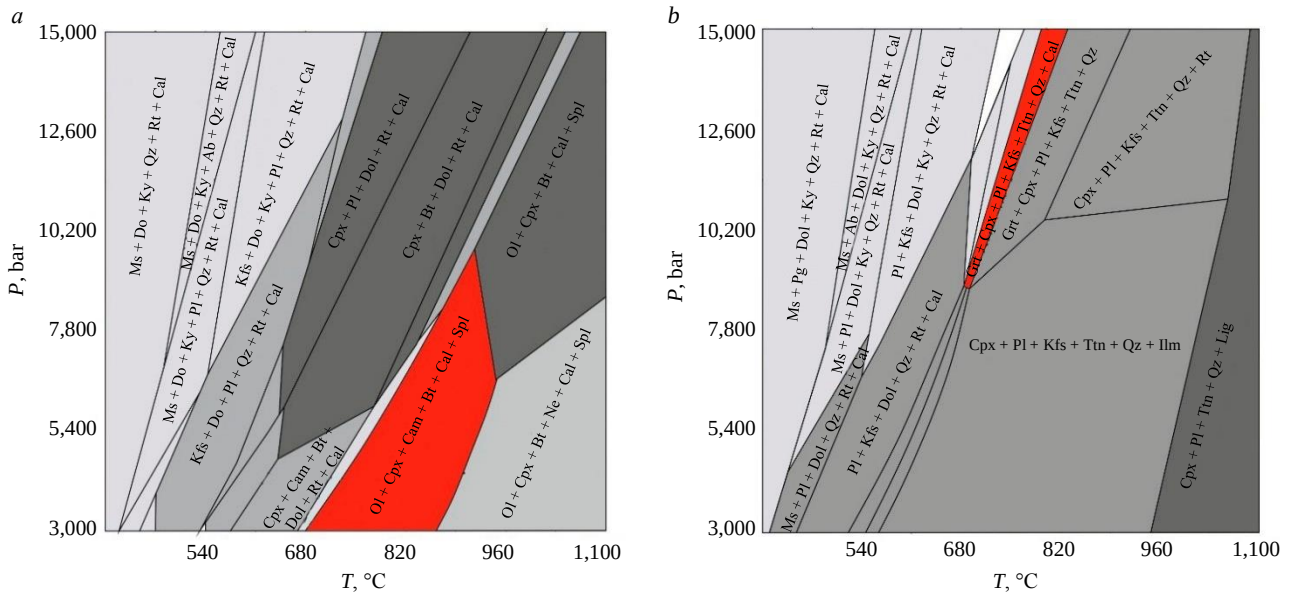


Fig.7. *P–T* pseudosections: *a* – for silicate marbles (sample 822013-1/2); *b* – for carbonate-silicate rocks (sample 822119-1/1). The field of the desired paragenesis is shown in red: Ol + Cpx + Cam + Bt + Cal + Spl for silicate marbles; Grt + Cpx + Pl + Kfs + Ttn + Qz + Cal for carbonate-silicate rocks

This is an open access article under the CC BY 4.0 license

In the pseudosection for a given composition of carbonate-silicate rocks (sample 822119-1/1, Fig.7, *b*), the stability field of the observed paragenesis Grt + Cpx + Pl + Kfs + Ttn + Qz + Cal is located in the region of significantly higher pressures (8-15 kbar) and somewhat lower temperatures (680-820 °C). At higher temperatures, calcite disappears, and at lower temperatures, rutile and dolomite appear. At lower pressures, associations with ilmenite are stable, and at higher pressures, with kyanite.

Discussion

Under conditions of high-temperature metamorphism of carbonate sediments with varying proportions of terrigenous admixture, rare mineral associations with forsterite, spinel, humite group minerals, etc. are formed [32]. However, similar mineral associations are also characteristic of magnesian skarns. Probably, both primary sedimentary carbonate-silicate rocks and metasomatic magnesian skarns are widely distributed in metamorphic complexes.

Primary sedimentary carbonate-silicate rocks are known within the Fennoscandian Shield – in the Ladoga region (Sortavala series) [33], as well as in the Belomorian mobile belt within the Lapland-Kolvitsky granulite belt [31, 34, 35]. Another example is the generally well-studied carbonate-silicate rocks of the Southern Urals. Thus, as a result of a detailed study of the carbonate-silicate rocks of the Ilmenogorsk complex, the authors came to the conclusion that these are primary sedimentary formations [36]. An example of metasomatic carbonate-silicate rocks are the formations of the Kusa-Kopansky complex, which were formed as a result of metasomatic reworking of dolomites, i.e. they are magnesian skarns [5]. The metasomatic nature of the vein carbonate-silicate rocks of the Tazheransky massif is beyond doubt [37]. Alternative hypotheses have also been put forward about the genesis of some carbonate-silicate rocks – individual occurrences in the Urals are considered carbonatite [38, 39], although this point of view is met with serious objections [5, 36]. For the early Precambrian carbonate-silicate rocks of the Okhotsk massif, the primary sedimentary nature is rejected, and on the basis of isotope-geochemical data, their deep, but not carbonatite nature is assumed – the existence of a deep fluid-carbonate mass is discussed [40]. The nature of the calciphyres of the Irkutsk block also appears ambiguous; they are considered both as products of metamorphism of calc-silicate sedimentary rocks [41] and as a result of metasomatism of carbonate rocks at contact with aluminosilicate rocks [42]. Nevertheless, the results of geochemical studies allow us to conclude that the formation of calciphyres of the Irkutsk block is associated with the metamorphism of terrigenous-carbonate sediments [1]. Thus, without a detailed mineralogical and petrographic study it is difficult or even impossible to judge the origin and geological evolution of carbonate-silicate rocks.

The first results of the study of two lenticular bodies of metacarbonate rocks within the Khapchan series showed that these rocks differ sharply in mineral and chemical composition, despite the common structural position and close spatial location. Metacarbonates of the first of the two lens-shaped bodies are represented by silicate marbles composed of calcite, dolomite, forsterite, clinohumite, spinel, enstatite, diopside, pargasite, meionite, and feldspars. Silicate marbles are heterogeneous – in varieties with clinohumite, fluoropargasite and fluorphlogopite appear, and the amount of forsterite decreases (up to its complete disappearance). Reaction structures are common in silicate marbles – replacement of enstatite and forsterite by diopside, development of dolomite rims around spinel and complex zonal rims around potassium feldspar, including plagioclase, diopside, and phlogopite. In addition, quartz veins are common in silicate marbles, surrounded by clinopyroxene rims, accumulations of phlogopite, feldspars, with a small amount of scapolite. Thus, within one thin section, quartz is found in association with forsterite, spinel and dolomite, but does not directly contact and is a later mineral. It is important to note that the silicate marbles contain fragments of host terrigenous rocks [13], preserved despite the high degree of metamorphic reworking and undoubtedly indicating the primary sedimentary nature of the silicate marbles. Their primary sedimentary nature is also confirmed by the fact that chaotic breccias with carbonate cement, related

This is an open access article under the CC BY 4.0 license

to the flysch-carbonate subtype of accretionary olistostrome, were found at the base of the Khapchan series section [13].

Metacarbonates of the second of the studied lenticular bodies are represented by carbonate-silicate rocks, the mineral composition of which differs significantly from silicate marbles. Carbonate-silicate rocks are composed of calcite, quartz, feldspars, diopside, grossular, marialite, and vesuvianite. No reaction structures were noted in these rocks. Their mineral composition differs – clinopyroxene is significantly more ferruginous, and potassium feldspar contains less Ba than in silicate marbles. There is also a difference in the REE distribution spectra. Clinopyroxene in carbonate-silicate rocks differs from clinopyroxene (both from primary porphyroblastic clinopyroxene in the rock matrix and from secondary clinopyroxene developing on forsterite) of silicate marbles by a higher REE content and a concave shape of the spectrum in the HREE region. Potassium feldspar from silicate marbles is significantly depleted in LREE compared to potassic feldspar from carbonate-silicate rocks, while the HREE content in all analyzed potassic feldspars is comparable. It is interesting to note the presence of a pronounced positive Eu anomaly in all analyzed potassic feldspars. This probably indicates that potassium feldspar was formed when there was no plagioclase in the metacarbonate rocks. Indeed, in silicate marbles, plagioclase is concentrated in reaction rims and in fringes around quartz veins. At the same time, in carbonate-silicate rocks, plagioclase is distributed in the matrix together with quartz and calcite – apparently, all three minerals were formed simultaneously. The composition of scapolite in silicate marbles and carbonate-silicate rocks differs in both major and minor elements. Meionite from silicate marbles is characterized by an increased LREE content, while marialite from carbonate-silicate rocks inherits the shape of the REE distribution spectrum of the potassium feldspar it replaces. Grossular from carbonate-silicate rocks is similar to skarn garnets in its rare-element composition and REE distribution spectrum [5].

The chemical composition of the rocks also contrasts in the two lenses. Carbonate-silicate rocks are significantly enriched in SiO_2, Al_2O_3, FeO, Na_2O, K_2O, TiO_2 and contain less MgO, CaO, than silicate marbles. A similar pattern – an increase in the content of SiO_2, FeO, a decrease in MgO, CaO – is observed in each of the two lenses from the center to the periphery. The observed variations in chemical composition are significantly wider than those typically found in primary sedimentary carbonate-silicate rocks [1, 34]. Although all the metacarbonate rocks studied are characterized by similar, flat REE distribution spectra, the REE content in carbonate-silicate rocks is an order of magnitude higher than in silicate marbles.

It is important to note the difference in *PT*-parameters obtained for silicate marbles (temperatures of 700-900 °C and pressures of no more than 8 kbar, which corresponds to the granulite facies of metamorphism) and for carbonate-silicate rocks (temperatures of 680-820 °C, pressures of 8-15 kbar, which corresponds to the amphibolite facies of metamorphism). Insufficient data on *PT*-parameters and evolution of metamorphism of the Khapchan series rocks do not allow us to reliably determine whether the difference in *PT*-parameters is related to heterogeneity of the degree of metamorphism within one event or to the relationship obtained with two different events. However, since the body of carbonate-silicate rocks is located near the Billyakh shear zone, while silicate marbles were studied at some distance from it (see Fig.1), it can be assumed that the observed differences in *PT*-parameters are related to local superimposed metamorphism and, probably, metasomatismin the Billyakh zone area.

It is believed that in the Khapchan SFZ (structural-formational zone), sedimentogenic deposits were metamorphosed under granulite facies conditions 1.97 billion years ago, and somewhat later locally underwent high-temperature metamorphism [43], the peak of which occurred in the period 1.91-1.92 billion years, which most strongly affected the rocks within the Billyakh suture (melange) zone [9]. The difference between carbonate-silicate rocks and silicate marbles in chemical and mineral composition can be largely explained by variations in the composition of the sedimentary protolith, assuming that in carbonate-silicate rocks the terrigenous admixture was predominant, while in silicate marbles it was insignificant. Considering the similarity of the REE distribution

This is an open access article under the CC BY 4.0 license

spectra, the primary sedimentary nature of carbonate-silicate rocks, as well as silicate marbles, is beyond doubt.

At the same time, a number of features indicate that the metacarbonate rocks were subjected to metasomatic reworking, probably during regional metamorphism, under the influence of fluid separated from the enclosing gneisses. Thus, in silicate marbles, reaction rims are observed around orthopyroxene, forsterite, potassium feldspar, as well as quartz veins bordered by accumulations of phlogopite, feldspars, and diopside. In carbonate-silicate rocks, the development of secondary marialite on potassium feldspar is revealed, and the rare-element composition of garnet may indicate its metasomatic origin. Therefore, further geological and petrological study of metacarbonate rocks is required in order to reconstruct their metamorphic history in more detail, as well as to establish the intensity of metasomatic processes and their role in the geological history of rocks.

Conclusion

In two lenticular bodies of metacarbonate rocks among the gneisses of the Khapchan series, significant differences in the mineral and chemical composition of the rocks were revealed: carbonate-silicate rocks are composed of calcite, quartz, feldspars, diopside, grossular, marialite, vesuvianite; silicate marbles are composed of calcite, dolomite, forsterite, clinohumite, spinel, enstatite, diopside, pargasite, meionite, feldspars. Carbonate-silicate rocks are significantly enriched in SiO_2, Al_2O_3, FeO, Na_2O, K_2O, TiO_2 and contain less MgO, CaO than silicate marbles.

The first assessments of *PT*-parameters revealed differences in definitions for silicate marbles (temperatures 700-900 °C and pressures no more than 8 kbar) and for carbonate-silicate rocks (temperatures 680-820 °C, pressures 8-15 kbar).

Silicate marbles have a primary sedimentary nature, as evidenced by their rare-element composition and the presence of fragments of gneisses. There is no doubt about the primary sedimentary nature of carbonate-silicate rocks, which are very similar in REE distribution spectra and rare-element composition to silicate marbles.

In silicate marbles, reaction rims around orthopyroxene, forsterite, potassium feldspar, and quartz veins bordered by accumulations of phlogopite, feldspar, and diopside are noted. In carbonate-silicate rocks, secondary marialite development is revealed on potassium feldspar. These features may indicate that metacarbonate rocks have undergone metasomatic reworking.

REFERENCES

1. Urmantseva L.N., Turkina O.M., Kapitonov I.N. Protoliths of Paleoproterozoic calciphyres from the Irkut block (*Sharyzhalgai uplift of the Siberian craton*): composition and origin. *Russian Geology and Geophysics*. 2012. Vol. 53. N 12, p. 1681-1697. DOI: 10.1016/j.rgg.2012.10.003

2. Rosen O.M., Andreev V.P., Belov A.N. et al. The Archaean of the Anabar shield and the problems of early evolution of the Earth. Moscow: Nauka, 1988, p. 253 (in Russian).

3. Abdrakhmanov I.A., Gulbin Yu.L., Gembitskaya I.M. Assemblage of Fe–Mg–Al–Ti–Zn Oxides in Granulites of the Bunger Hills, East Antarctica: Evidence of Ultrahigh-Temperature Metamorphism. *Geology of Ore Deposits*. 2022. Vol. 64. N 8, p. 519-549. DOI: 10.1134/S1075701522080025

4. Salimgaraeva L.I., Berezin A.V. Garnetites from Marun-Keu eclogite complex (Polar Urals): geochemistry and the problem of genesis. *Journal of Mining Institute.* 2023. Vol. 262, p. 509-525.

5. Stativko V.S., Skublov S.G., Smolenskiy V.V., Kuznetsov A.B. Trace and rare-earth elements in garnets from silicate-carbonate formations of the Kusa-Kopan complex (Southern Urals). *Lithosphere.* 2023. Vol. 23. N 2, p. 225-246 (in Russian). DOI: 10.24930/1681-9004-2023-23-2-225-246

6. Skublov S.G., Levashova E.V., Mamykina M.E. et al. The polyphase Belokurikhinsky granite massif, Gorny Altai: isotope-geochemical study of zircon. *Journal of Mining Institute.* 2024. Vol. 268, p. 552-575.

7. Levashova E.V., Mamykina M.E., Skublov S.G. et al. Geochemistry (TE, REE, Oxygen) of Zircon from Leucogranites of the Belokurikhinsky Massif, Gorny Altai, as Indicator of Formation Conditions. *Geochemistry International*. 2023. Vol. 61. N 13, p. 1323-1339. DOI: 10.1134/S001670292311006X

8. Skublov S.G., Petrov D.A., Galankina O.L. et al. Th-Rich Zircon from a Pegmatite Vein Hosted in the Wiborg Rapakivi Granite Massif. *Geosciences*. 2023. Vol. 13. Iss. 12. N 362. DOI: 10.3390/geosciences13120362

9. Gosudarstvennaya geologicheskaya karta Rossiiskoi Federatsii. Masshtab 1:1,000,000 (trete pokolenie). List R-49 – Olenek. Obyasnitelnaya zapiska. St. Petersburg: Kartograficheskaya fabrika VSEGEI, 2016, p. 448.

This is an open access article under the CC BY 4.0 license

10. Gusev N.I., Sergeeva L.Yu., Skublov S.G. Evidence of Subduction of the Paleoproterozoic Oceanic Crust in the Khapchan Belt of the Anabar Shield, Siberian Craton. *Petrology*. 2021. Vol. 29. N 2, p. 95-113. DOI: 10.1134/S0869591121020041

11. Yurchenko A.V., Skublov S.G., Gusev N.I., Romanova L.Yu. Mineral composition and parameters of metamorphism of granulite in the Khapchan orogenic belt (Anabar shield). *Zapiski Rossiiskogo mineralogicheskogo obshchestva*. 2024. Vol. 153. N 5, p. 13-37 (in Russian). DOI: 10.31857/S0869605524050021

12. Zlobin V.L., Rosen O.M., Abbyasov A.A. Two Meta-Sedimentary Basins in the Early Precambrian Granulites of the Anabar Shield (Polar Siberia): Normative Mineral Compositions Calculated by the MINLITH Program and Basin Facies Interpretations. Precambrian Sedimentary Environments: A Modern Approach to Ancient Depositional Systems. Blackwell Science, 2002, p. 275-291. DOI: 10.1002/9781444304312.ch12

13. Gusev N.I., Romanova L.Y., Skublov S.G. Geochemistry and age of zircon from Khapchan accretional olistostrom of Anabar shield. Geologiya i mineralno-syrevye resursy Severo-Vostoka Rossii 2024: Materialy XIV Mezhdunarodnoi nauchno-prakticheskoi konferentsii, posvyashchennoi 300-letiyu Rossiiskoi akademii nauk i 100-letiyu zolotodobyvayushchei promyshlennosti Respubliki Sakha (Yakutiya), 26-29 March 2024, Yakutsk, Russia. Novosibirsk: Sibirskoe otdelenie RAN, 2024, p. 302-308 (in Russian). DOI: 10.53954/9785604990100_302

14. Gosudarstvennaya geologicheskaya karta SSSR. Masshtab 1:200,000. Seriya Anabarskaya. Listy R-49-XXIII, XXIV. Moscow: Glavnoe upravlenie geodezii i kartografii Gosudarstvennogo geologicheskogo komiteta SSSR, 1965.

15. Pourmand A., Dauphas N., Ireland T.J. A novel extraction chromatography and MC-ICP-MS technique for rapid analysis of REE, Sc and Y: Revising CI-chondrite and Post-Archean Australian Shale (PAAS) abundances. *Chemical Geology*. 2012. Vol. 291, p. 38-54. DOI: 10.1016/j.chemgeo.2011.08.011

16. Bulakh A.G., Zolotarev A.A., Krivovichev V.G. Structure, isomorphism, formulas, and classification of minerals. St. Petersburg: Izd-vo Sankt-Peterburgskogo gosudarstvennogo universiteta, 2014, p. 132.

17. Locock A.J. An Excel spreadsheet to classify chemical analyses of amphiboles following the IMA 2012 recommendations. *Computers & Geosciences*. 2014. Vol. 62, p. 1-11. DOI: 10.1016/j.cageo.2013.09.011

18. Whitney D.L., Evans B.W. Abbreviations for names of rock-forming minerals. *American Mineralogist*. 2010. Vol. 95. N 1, p. 185-187. DOI: 10.2138/am.2010.3371

19. McDonough W.F., Sun S.S. The composition of the Earth. *Chemical Geology*. 1995. Vol. 120. Iss. 3-4, p. 223-253. DOI: 10.1016/0009-2541(94)00140-4

20. Connolly J.A.D. Computation of phase equilibria by linear programming: A tool for geodynamic modeling and its application to subduction zone decarbonation. *Earth and Planetary Science Letters*. 2005. Vol. 236. Iss. 1-2, p. 524-541. DOI: 10.1016/j.epsl.2005.04.033

21. Holland T., Powell R. A Compensated-Redlich-Kwong (CORK) equation for volumes and fugacities of CO_2 and H_2O in the range 1 bar to 50 kbar and 100-1,600 °C. *Contributions to Mineralogy and Petrology*. 1991. Vol. 109. Iss. 2, p. 265-273. DOI: 10.1007/BF00306484

22. Holland T.J.B., Powell R. An internally consistent thermodynamic data set for phases of petrological interest. *Journal of Metamorphic Geology*. 1998. Vol. 16. Iss. 3, p. 309-343. DOI: 10.1111/j.1525-1314.1998.00140.x

23. Rosen O.M., Fettes D., Desmons J. Chemical and mineral compositions of metacarbonate rocks under regional metamorphism conditions and guidelines on rock classification. *Russian Geology and Geophysics*. 2005. Vol. 46. N 4, p. 351-360.

24. Condie K.C., Wilks M., Rosen O.M., Zlobin V.L. Geochemistry of metasediments from the Precambrian Hapschan Series, eastern Anabar Shield, Siberia. *Precambrian Research*. 1991. Vol. 50. Iss. 1-2, p. 37-47. DOI: 10.1016/0301-9268(91)90046-D

25. Kamkicheva O.N., Voznaya A.A., Mikhailova T.V., Gribanova G.I. Resource Approach to the Estimation of International Cooperation in Integrated Development of Calciphyre Deposits. Proceedings of the 8th Russian-Chinese Symposium "Coal in the 21st Century: Mining, Processing, Safety", 10-12 October 2016, Kemerovo, Russia. Atlantis Press, 2016, p. 1-4. DOI: 10.2991/coal-16.2016.1

26. Morimoto N., Fabries J., Ferguson A.K. et al. Nomenclature of Pyroxenes. *Mineralogical Magazine*. 1988. Vol. 52. Iss. 367, p. 535-550. DOI: 10.1180/minmag.1988.052.367.15

27. Rieder M., Cavazzini G., Dyakonov Yu.S. et al. Nomenclature of the micas. *The Canadian Mineralogist*. 1998. Vol. 36. N 3, p. 905-912.

28. Hawthorne F.C., Oberti R., Harlow G.E. et al. Nomenclature of the amphibole supergroup. *American Mineralogist*. 2012. Vol. 97. N 11-12, p. 2031-2048. DOI: 10.2138/am.2012.4276

29. Grew E.S., Locock A.J., Mills S.J. et al. Nomenclature of the garnet supergroup. *American Mineralogist*. 2013. Vol. 98. N 4, p. 785-811. DOI: 10.2138/am.2013.4201

30. Bosi F., Biagioni C., Pasero M. Nomenclature and classification of the spinel supergroup. *European Journal of Mineralogy*. 2019. Vol. 31. N 1, p. 183-192. DOI: 10.1127/ejm/2019/0031-2788

31. Krylov D.P., Klimova E.V. Origin of carbonate-silicate rocks of the Porya Guba (the Lapland-Kolvitsa Granulite Belt) revealed by stable isotope analysis ($\delta^{18}O$, $\delta^{13}C$). *Journal of Mining Institute.* 2024. Vol. 265, p. 3-15.

32. Pertsev N.N. High-temperature metamorphism and metasomatism of carbonate rocks. Moscow: Nauka, 1977, p. 256.

33. Kuznetsov A.B., Gorokhov I.M., Azimov P.Ya., Dubinina E.O. Sr- and C-Chemostratigraphy Potential of the Paleoproterozoic Sedimentary Carbonates under Medium-Temperature Metamorphism: the Ruskeala Marble, Karelia. *Petrology*. 2021. Vol. 29. N 2, p. 175-194. DOI: 10.1134/S0869591121010033

34. Safronov V.T., Rosen O.M. Metacarbonate Rocks (Calciphyres) of the Lapland–Kolvitsa Granulite Belt, Baltic Shield. *Lithology and Mineral Resources.* 2004. Vol. 39. N 5, p. 425-436. DOI: 10.1023/B:LIMI.0000040733.81697.5a

35. Levitskiy V.I., Reznitsky L.Z., Levitskiy I.V. Geochemistry of Carbonate Rocks in the Early Precambrian and Phanerozoic Metamorphic Complexes of East Siberia, North-West Russia, and Pamirs. *Geochemistry International.* 2019. Vol. 57. N 4, p. 438-455. DOI: 10.1134/S0016702919040074

36. Valizer P.M., Cherednichenko S.V., Krasnobaev A.A. Mineralogy, geochemistry and age of metacarbonate-silicate rocks of the Ilmenogorsky complex. *Litosfera.* 2019. Vol. 19. N 1, p. 92-110 (in Russian). DOI: 10.24930/1681-9004-2019-19-1-92-110

37. Starikova A.E., Sklyarov E.V., Kotov A.B. et al. Vein Calciphyre and Contact Mg Skarn from the Tazheran Massif (Western Baikal area, Russia): Age and Genesis. *Doklady Earth Sciences.* 2014. Vol. 457. Part 2, p. 1003-1007. DOI: 10.1134/S1028334X14080182

38. Korinevsky V.G., Korinevsky E.V. New type of carbonatites in the Urals. *Litosfera*. 2013. N 3, p. 43-56 (in Russian).

This is an open access article under the CC BY 4.0 license

39. Popov V.A., Makagonov E.P., Nikandrov S.N. About new settings of carbonatites on the Urals. *Uralskii mineralogicheskii sbornik.* 1998. N 8, p. 134-148 (in Russian).

40. Lokhov K.I., Prasolov E.M., Kapitonov I.N. et al. Isotope geology of early Precambrian calciphyres of the Okhotsk massif (North-East of Russia). *Regionalnaya geologiya i metallogeniya*. 2008. N 35, p. 56-71.

41. Geologiya granulitov. Putevoditel Baikalskoi ekskursii mezhdunarodnogo simpoziuma v ramkakh proektov "Geokhimiya arkheya" i "Metallogeniya dokembriya". Irkutsk: Vostochno-Sibirskii filial Sibirskogo otdeleniya AN SSSR, 1981, p. 97.

42. Levitsky V.I. Petrology and geochemistry of metasomatism on continental crust formation. Novosibirsk: Geo, 2005, p. 340.

43. Skublov S.G., Gusev N.I., Salimgaraeva L.I., Romanova L.Yu. Trace Element Composition of Discordant Zircon as a Reflection of the Fluid Regime of Paleoproterozoic Granulite Metamorphism (Khapchan Terrane, Anabar Shield). *Geochemistry International.* 2024. Vol. 62. N 8, p. 793-804. DOI: 10.1134/S0016702924700393

***Authors*: Ekaterina Yu. Akimova,** *Candidate of Geological and Mineralogical Sciences, Senior Lecturer, e.akimova@spbu.ru, https://orcid.org/0000-0002-7816-7754* (*Saint Petersburg State University, Saint Petersburg, Russia*), **Nikolai I. Gusev,** *Head of Department, https://orcid.org/0000-0002-3461-0961* (*All-Russian Geological Research Institute of A.P.Karpinsky, Saint Petersburg, Russia*; *Institute of Precambrian Geology and Geochronology RAS, Saint Petersburg, Russia*), **Aleksandr D. Savelev,** *Candidate of Geological and Mineralogical Sciences, Leading Geologist, https://orcid.org/0000-0002-8120-3576* (*Saint Petersburg State University, Saint Petersburg, Russia*; *All-Russian Geological Research Institute of A.P.Karpinsky, Saint Petersburg, Russia*), **Daniil R. Donchenko,** *Postgraduate Student, https://orcid.org/0009-0004-9664-4958* (*Saint Petersburg State University, Saint Petersburg, Russia*).

The authors declare no conflict of interests.

This is an open access article under the CC BY 4.0 license